Robust Position Tracking of a Palletizer Robot Using Super-Twisting Higher-Order Sliding Mode Control

Amirz Feizizadeh

Abstract: **This paper investigates robust trajectory tracking of a three-degree-of-freedom palletizer robot in the presence of dynamic-model uncertainty and matched disturbances. A nonlinear robot model is formulated in standard manipulator form using the Lagrangian approach. A conventional first-order sliding-mode controller is first considered as a benchmark, followed by a second-order super-twisting controller designed to reduce the chattering associated with discontinuous control. The proposed controller employs a proportional sliding surface and a square-root nonlinear feedback term with an auxiliary discontinuous state. Under bounded and Lipschitz-continuous matched uncertainties, finite-time convergence of the sliding variable is established using a Lyapunov-based argument. MATLAB/Simulink simulations with sinusoidal joint references and a 20% dynamic-model mismatch are used to evaluate the controllers. The results demonstrate accurate joint-position tracking and smoother control inputs with the super-twisting scheme compared with conventional sliding-mode control. End-effector trajectories are also evaluated to assess the resulting Cartesian tracking performance. The study provides a simulation-based assessment of super-twisting control for robust motion control of nonlinear palletizing manipulators.**

Keywords: **Palletizer robot, sliding-mode control, super-twisting algorithm, trajectory tracking, model uncertainty.**

I Introduction

Industrial robotic manipulators are widely used in manufacturing operations that require repeatability, speed, precision, and autonomous motion [1]-[3]. Palletizing is a representative application in which a robot repeatedly transfers products from a production line to prescribed locations on a pallet. The dynamic behavior of a palletizer is nonlinear and coupled because the motion of one joint influences the dynamic loads associated with the remaining joints [4]. Consequently, accurate trajectory tracking requires a control strategy that can cope with nonlinear coupling, uncertainty in physical parameters, payload variations, unmodeled dynamics, and external disturbances.

The dynamics of a rigid robotic manipulator can be expressed in the standard form

$$M(q)\ddot{q} + C(q,\dot{q})\dot{q} + \mathcal{G}(q) = \tau + d \tag{1}$$

where $q \in \mathbb{R}^n$ denotes the joint-position vector, $M(q)$ is the positive-definite inertia matrix, $C(q,\dot{q})\dot{q}$ represents Coriolis and centrifugal effects, $\mathcal{G}(q)$ is the gravity vector, τ is the actuator torque vector, and d represents external disturbances and unmodeled dynamics. For the considered palletizer, the underlying dynamic model was obtained from kinetic and potential energies using the Lagrange formulation.

The control of uncertain nonlinear mechanical systems is challenging because errors in inertia, link masses, inertial parameters, friction, and payload can propagate through the nonlinear equations and appear directly as tracking errors [5]-[8]. Sliding-mode control (SMC) is attractive in this context because its switching mechanism provides robustness against an important class of matched uncertainties [9], [10]. The conventional approach, however, contains a discontinuous feedback term. Under finite sampling frequency and nonideal actuators, this term leads to high-frequency oscillations commonly known as chattering [11]-[14].

Higher-order sliding-mode (HOSM) control preserves the robustness concept of SMC while enforcing the sliding condition on higher derivatives of the sliding variable. Levant established a general framework for higher-order sliding algorithms and demonstrated their robustness properties [15]. A comprehensive treatment of HOSM control, observation, and implementation can be found in [16]. Among the HOSM methods, the super-twisting algorithm is especially relevant to mechanical systems because the control input can remain continuous even though a discontinuous signal is used in the internal controller dynamics [17].

Second-order sliding-mode methods have been investigated for robotic manipulators. Capisani *et al.* developed and experimentally validated a second-order sliding-mode motion controller for robot manipulators [18]. More recently, super-twisting approaches have been studied for two-link manipulators, including optimization-based gain tuning [19]. Adaptive super-twisting methods have also been developed for robotic manipulators with actuator faults [20] and input saturation [21]. Experimental results on a three-degree-of-freedom Delta parallel robot have further demonstrated the practical potential of adaptive feedforward super-twisting control [22].

Manuscript received 7 October, 2026; revised 28 October, 2026; accepted 3 November, 2026.

A. Feizizadeh is with the department of electrical engineering, Quchan University of Technology, Quchan 94771-67335, Iran (e-mail: feizizadeh.amir@gmail.com).

The present study focuses on a different industrially motivated platform: the ROBO-ARM V01 palletizer. The underlying work models the robot as a three-degree-of-freedom, nine-link system and derives its nonlinear dynamics before comparing conventional SMC with a higher-order super-twisting controller. The study explicitly considers external disturbances and internal uncertainty, derives the controller analytically, investigates stability, and evaluates the response through MATLAB/Simulink simulations.

The main contributions of this manuscript are summarized as follows:

1) A complete nonlinear dynamic model of the ROBO-ARM V01 palletizer is formulated in standard manipulator form using the Lagrangian approach. The model captures the coupled, nonlinear dynamics of the nine-link mechanical structure and is intentionally mismatched with respect to the parameter uncertainty.
2) A super-twisting higher-order sliding-mode controller is developed using a proportional sliding surface, a square-root nonlinear feedback term, and an auxiliary discontinuous internal state. This formulation preserves the robustness of conventional sliding-mode control while allowing the actuator torque to remain continuous under ideal continuous-time conditions, thereby reducing chattering.
3) A rigorous finite-time stability argument is established for the closed-loop super-twisting sliding dynamics. Under standard boundedness and Lipschitz-continuity assumptions on the lumped matched uncertainty and its derivative, a quadratic Lyapunov function is constructed using a transformed state variable, and sufficient gain conditions are derived to guarantee finite-time convergence of the sliding variable to zero.

The remainder of this paper is organized as follows. Section II presents the robot model and the control problem. Section III develops the conventional and super-twisting controllers. Section IV presents the simulation configuration and results. Section V concludes the paper.

II Robot Modeling and Problem Formulation

A Robot configuration

The considered ROBO-ARM V01 palletizer is a laboratory-scale industrial manipulator with three actuated degrees of freedom and nine mechanical links. The mechanical dimensions, masses, and inertia properties are obtained from the robot CAD model used in the underlying study. The three generalized coordinates are collected as

$$q = \begin{bmatrix} q_1 & q_2 & q_3 \end{bmatrix}^T \qquad \dot{q} = \begin{bmatrix} \dot{q}_1 & \dot{q}_2 & \dot{q}_3 \end{bmatrix}^T \tag{2}$$

The coordinate transformations are constructed from elementary rotation matrices. For example, a representative set of transformations is

$$R_z(q_1) = \begin{bmatrix} \cos q_1 & -\sin q_1 & 0 \\ \sin q_1 & \cos q_1 & 0 \\ 0 & 0 & 1 \end{bmatrix} \tag{3}$$

$$R_x(q_2) = \begin{bmatrix} 1 & 0 & 0 \\ 0 & \cos q_2 & -\sin q_2 \\ 0 & \sin q_2 & \cos q_2 \end{bmatrix} \tag{4}$$

$$R_x(q_3) = \begin{bmatrix} 1 & 0 & 0 \\ 0 & \cos q_3 & -\sin q_3 \\ 0 & \sin q_3 & \cos q_3 \end{bmatrix} \tag{5}$$

The complete transformation chain is obtained by composing the appropriate rotations and translations associated with the actual link geometry.

B Energy formulation and dynamic equations

The kinetic energy of a rigid-link manipulator can be written as

$$T = \sum_{i=1}^{N} \left[\frac{1}{2} m_i v_{c_i}^T v_{c_i} + \frac{1}{2} \omega_i^T I_i \omega_i \right] \tag{6}$$

where m_i, v_{c_i}, I_i, and ω_i denote the mass, center-of-mass linear velocity, inertia tensor, and angular velocity of link i, respectively. The gravitational potential energy is

$$U = \sum_{i=1}^{N} m_i g^T r_{c_i} \tag{7}$$

The Lagrangian function is

$$L = T - U \tag{8}$$

The Euler–Lagrange equations are then given by

$$\frac{d}{dt}\left(\frac{\partial L}{\partial \dot{q}}\right) - \frac{\partial L}{\partial q} = \tau \tag{9}$$

The final manipulator model is expressed as

$$\tau = M(q)\ddot{q} + V(q, \dot{q}) \tag{10}$$

where

$$V(q, \dot{q}) = C(q, \dot{q})\dot{q} + \mathcal{G}(q) \tag{11}$$

The matrix $M(q) \in \mathbb{R}^{3\times 3}$ is symmetric and positive definite for nonsingular configurations. The detailed symbolic entries of $M(q)$ and $V(q, \dot{q})$ are lengthy and depend on the nine-link geometry; they are therefore better placed in supplementary material or an appendix in the final journal submission.

C Uncertain model

In practice, the dynamic model is not known exactly because of parameter mismatch, payload changes, friction, unmodeled effects, and external disturbances. We therefore distinguish the nominal model used by the controller from the actual plant model:

$$\hat{M}(q) = M(q) + \Delta M(q) \tag{12}$$

$$\hat{V}(q, \dot{q}) = V(q, \dot{q}) + \Delta V(q, \dot{q}) \tag{13}$$

TABLE 1. Representative robot and simulation parameters used.

Parameter	Value/description
Robot	ROBO-ARM V01 palletizer
Degrees of freedom	3
Number of links	9
Dynamic formulation	Lagrangian
Simulation platform	MATLAB/Simulink
Nominal model mismatch	20%
Initial position	$[0\ \ 0.5\ \ 1]^T$ rad
Baseline SMC interval	5 s
Super-twisting interval	20 s

The plant is modeled by

$$M(q)\ddot{q} + V(q,\dot{q}) = \tau + d(t) \tag{14}$$

where $d(t)$ is a lumped matched disturbance.

For the simulation study, the nominal dynamic model is intentionally mismatched with respect to the plant. The source work uses a 20% model perturbation, represented by the nominal matrices as approximately 0.8 times the actual matrices. This construction provides a direct test of the robustness of the controller.

D Tracking objective

Let $q_d(t)$ denote the desired trajectory and define the tracking error, for this manuscript, as

$$e = q - q_d \tag{15}$$

The sign convention in (15) is sign-equivalent to the source thesis notation $e = q_d - q$ and is adopted here to obtain the standard sliding-surface form. The control objective is

$$\lim_{t\to\infty} e(t) = 0 \tag{16}$$

with fast convergence and robust performance under bounded uncertainties and disturbances.

III Control Design Based on Sliding Modes

A First-order sliding-mode benchmark

A conventional sliding surface is selected as

$$s = \dot{e} + \Lambda e \tag{17}$$

where

$$\Lambda = \mathrm{diag}(\lambda_1, \lambda_2, \lambda_3), \quad \lambda_i > 0 \tag{18}$$

When $s = 0$, the tracking-error dynamics satisfy

$$\dot{e} + \Lambda e = 0 \tag{19}$$

which yields exponentially decaying tracking errors.

Define the reference acceleration

$$\ddot{q}_r = \ddot{q}_d - \Lambda\dot{e} \tag{20}$$

A conventional model-based SMC law is then

$$\tau_{\mathrm{SMC}} = \hat{M}(q)\ddot{q}_r + \hat{V}(q,\dot{q}) - \kappa\ \mathrm{sgn}(s) \tag{21}$$

where $\kappa = \mathrm{diag}(\kappa_1, \kappa_2, \kappa_3)$ is a positive switching-gain matrix. The switching term provides the robustness required to overcome bounded matched uncertainty. The main practical limitation of (21) is the direct discontinuity of the actuator signal.

B Super-twisting controller and its stability proof

The super-twisting algorithm is a second-order sliding-mode method that acts on the sliding variable and its derivative while avoiding a direct discontinuity in the actuator torque. Define

$$\mathrm{sig}^{\alpha}(s) = |s|^{\alpha}\,\mathrm{sgn}(s) \tag{22}$$

For $\alpha = 1/2$,

$$\mathrm{sig}^{1/2}(s) = |s|^{1/2}\,\mathrm{sgn}(s) \tag{23}$$

the proposed controller is given by

$$\tau_{\mathrm{ST}} = \hat{M}(q)\left[\ddot{q}_d - \Lambda\dot{e} - \kappa_1\,\mathrm{sig}^{1/2}(s) - z\right] + \hat{V}(q,\dot{q}) \tag{24}$$

with the auxiliary internal state governed by

$$\dot{z} = \kappa_2\,\mathrm{sgn}(s) \tag{25}$$

The diagonal gain matrices satisfy

$$\begin{aligned}\kappa_1 &= \mathrm{diag}(\kappa_{11}, \kappa_{12}, \kappa_{13}) > 0\\ \kappa_2 &= \mathrm{diag}(\kappa_{21}, \kappa_{22}, \kappa_{23}) > 0\end{aligned} \tag{26}$$

The controller in (24) is written with the error definition $e = q - q_d$. If the source notation $e = q_d - q$ is retained instead, the signs of the corresponding tracking and feedback terms must be changed consistently; the two conventions are mathematically equivalent when used consistently.

The significance of the super-twisting design is that the discontinuous sign function enters the internal state derivative rather than the actuator torque. Therefore the actual torque can be continuous under ideal continuous-time assumptions. This property makes the method attractive for mechanical actuators and has been studied extensively in robotic systems [20], [21]. Using (17), the derivative of the sliding variable is

$$\dot{s} = \ddot{q} - \ddot{q}_d + \Lambda\dot{e} \tag{27}$$

Substituting the plant model (14) and the controller (24), the resulting sliding dynamics can be collected in the generic form

$$\dot{s} = -\kappa_1\,\mathrm{sig}^{1/2}(s) - z + \Delta(t) \tag{28}$$

$$\dot{z} = \kappa_2\,\mathrm{sgn}(s) \tag{29}$$

where $\Delta(t)$ represents the lumped residual uncertainty defined by $\Delta(t) = M^{-1}(q)\left[\Delta M(q)\ddot{q}_r + \Delta V(q,\dot{q}) + d(t)\right]$. Depending on the sign convention used for the auxiliary state, an equivalent representation may contain a minus sign in (28); the stability argument is unchanged when the gain convention is chosen consistently.

Assume that the residual matched uncertainty is bounded and has a bounded derivative, i.e.,

$$\begin{aligned}|\Delta_i(t)| &\le \bar{\Delta}_i\\ \left|\dot{\Delta}_i(t)\right| &\le \mathcal{L}_i\end{aligned} \tag{30}$$

where $\bar{\Delta}_i$ and $\mathcal{L}_i$ are finite positive constants. These are standard assumptions in super-twisting analysis and are also used in recent manipulator applications [17], [20].

Define the transformed state vector

$$\xi = \begin{bmatrix} \xi_1 \\ \xi_2 \end{bmatrix} = \begin{bmatrix} |s|^{1/2}\operatorname{sgn}(s) \\ z - \Delta(t) \end{bmatrix} \tag{31}$$

This transformation is well-defined for all $s \in \mathbb{R}$ and maps the sliding dynamics into a homogeneous form. The choice of $\xi_2 = z - \Delta(t)$ accounts for the effect of the uncertainty on the auxiliary state and is essential for constructing a valid Lyapunov function.

The time derivative of ξ is computed as follows. For ξ_1,

$$\dot{\xi}_1 = \frac{1}{2}|s|^{-1/2}\dot{s} \tag{32}$$

$$= \frac{1}{2|s|^{1/2}}\left(-\kappa_1|s|^{1/2}\operatorname{sgn}(s) - z + \Delta(t)\right) \tag{33}$$

Using the definitions of ξ_1 and ξ_2, this becomes

$$\dot{\xi}_1 = \frac{1}{2|\xi_1|}\left(-\kappa_1\xi_1 - \xi_2\right) \tag{34}$$

$$= -\frac{\kappa_1}{2}\operatorname{sgn}(\xi_1) - \frac{\xi_2}{2|\xi_1|} \tag{35}$$

For ξ_2,

$$\dot{\xi}_2 = \dot{z} - \dot{\Delta}(t) \tag{36}$$

$$= \kappa_2\operatorname{sgn}(s) - \dot{\Delta}(t) \tag{37}$$

Since $\operatorname{sgn}(s) = \operatorname{sgn}(\xi_1)$ for $\xi_1 \neq 0$, this yields

$$\dot{\xi}_2 = \kappa_2\operatorname{sgn}(\xi_1) - \dot{\Delta}(t) \tag{38}$$

The transformed dynamics can therefore be written in the compact form

$$\dot{\xi} = \frac{1}{|\xi_1|}\mathcal{A}\xi + \mathcal{B}\dot{\Delta}(t) \tag{39}$$

where

$$\mathcal{A} = \begin{bmatrix} -\dfrac{\kappa_1}{2} & -\dfrac{1}{2} \\ \kappa_2 & 0 \end{bmatrix}, \quad \mathcal{B} = \begin{bmatrix} 0 \\ -1 \end{bmatrix} \tag{40}$$

This representation is valid for $\xi_1 \neq 0$, i.e., $s \neq 0$. The case $s = 0$ is addressed below.

Consider the quadratic Lyapunov function

$$W = \xi^T\mathcal{P}\xi \tag{41}$$

where $\mathcal{P}$ is a symmetric positive-definite matrix to be determined. The time derivative of W along the trajectories of (39) is

$$\dot{W} = \dot{\xi}^T\mathcal{P}\xi + \xi^T\mathcal{P}\dot{\xi} \tag{42}$$

$$= \frac{1}{|\xi_1|}\xi^T\left(\mathcal{A}^T\mathcal{P} + \mathcal{P}\mathcal{A}\right)\xi + 2\xi^T\mathcal{P}\mathcal{B}\dot{\Delta}(t) \tag{43}$$

For the unperturbed system (i.e., $\dot{\Delta}(t) = 0$), the derivative of W is negative definite if

$$\mathcal{A}^T\mathcal{P} + \mathcal{P}\mathcal{A} < 0 \tag{44}$$

The matrix $\mathcal{A}$ is Hurwitz if and only if $\kappa_1 > 0$ and $\kappa_2 > 0$. For any such gains, there exists a unique positive-definite matrix $\mathcal{P}$ satisfying the Lyapunov equation

$$\mathcal{A}^T\mathcal{P} + \mathcal{P}\mathcal{A} = -Q \tag{45}$$

for any chosen positive-definite matrix Q. A convenient choice is $Q = I$, which yields a unique solution $\mathcal{P} = \mathcal{P}^T > 0$. The existence of such a $\mathcal{P}$ is guaranteed by the Lyapunov theorem for linear time-invariant systems.

Substituting (45) into (43) gives

$$\dot{W} = -\frac{1}{|\xi_1|}\xi^TQ\xi + 2\xi^T\mathcal{P}\mathcal{B}\dot{\Delta}(t) \tag{46}$$

The perturbation term is bounded as follows. Since $|\dot{\Delta}(t)| \leq \mathcal{L}$,

$$2\xi^T\mathcal{P}\mathcal{B}\dot{\Delta}(t) \leq 2\mathcal{L}\left|\xi^T\mathcal{P}\mathcal{B}\right| \tag{47}$$

$$\leq 2\mathcal{L}\|\mathcal{P}\mathcal{B}\|\,\|\xi\| \tag{48}$$

Using $\|\xi\| \leq \dfrac{W^{1/2}}{\lambda_{\min}^{1/2}(\mathcal{P})}$, where $\lambda_{\min}(\mathcal{P})$ denotes the minimum eigenvalue of $\mathcal{P}$, we obtain

$$2\xi^T\mathcal{P}\mathcal{B}\dot{\Delta}(t) \leq \frac{2\mathcal{L}\|\mathcal{P}\mathcal{B}\|}{\lambda_{\min}^{1/2}(\mathcal{P})}W^{1/2} \tag{49}$$

Using the bound (49) in (46), we obtain

$$\dot{W} \leq -\frac{\lambda_{\min}(Q)}{|\xi_1|}\|\xi\|^2 + \frac{2\mathcal{L}\|\mathcal{P}\mathcal{B}\|}{\lambda_{\min}^{1/2}(\mathcal{P})}W^{1/2} \tag{50}$$

Since $|\xi_1| = |s|^{1/2}$ and $\|\xi\|^2 = |s| + \xi_2^2$, we have $\dfrac{\|\xi\|^2}{|\xi_1|} \geq |\xi_1| = |s|^{1/2}$. Moreover, $W = \xi^T\mathcal{P}\xi \leq \lambda_{\max}(\mathcal{P})\|\xi\|^2$, so $\|\xi\|^2 \geq \dfrac{W}{\lambda_{\max}(\mathcal{P})}$. Combining these inequalities yields

$$\frac{\|\xi\|^2}{|\xi_1|} \geq \frac{W}{\lambda_{\max}(\mathcal{P})\,|\xi_1|} \tag{51}$$

However, a more direct bound is obtained by noting that $|\xi_1| \leq \|\xi\| \leq \dfrac{W^{1/2}}{\lambda_{\min}^{1/2}(\mathcal{P})}$, which gives $\dfrac{1}{|\xi_1|} \geq \dfrac{\lambda_{\min}^{1/2}(\mathcal{P})}{W^{1/2}}$. Substituting this into (50),

$$\dot{W} \leq -\frac{\lambda_{\min}(Q)\,\lambda_{\min}^{1/2}(\mathcal{P})}{W^{1/2}}\|\xi\|^2 + \frac{2\mathcal{L}\|\mathcal{P}\mathcal{B}\|}{\lambda_{\min}^{1/2}(\mathcal{P})}W^{1/2} \tag{52}$$

Using $\|\xi\|^2 \geq \dfrac{W}{\lambda_{\max}(\mathcal{P})}$, we obtain

$$\dot{W} \leq -\left(\frac{\lambda_{\min}(Q)\,\lambda_{\min}^{1/2}(\mathcal{P})}{\lambda_{\max}(\mathcal{P})} - \frac{2\mathcal{L}\|\mathcal{P}\mathcal{B}\|}{\lambda_{\min}^{1/2}(\mathcal{P})}\right)W^{1/2} \tag{53}$$

Define the constant

$$c = \frac{\lambda_{\min}(Q)\,\lambda_{\min}^{1/2}(\mathcal{P})}{\lambda_{\max}(\mathcal{P})} - \frac{2\mathcal{L}\|\mathcal{P}\mathcal{B}\|}{\lambda_{\min}^{1/2}(\mathcal{P})} \tag{54}$$

If the gains κ_1 and κ_2 are chosen such that $\sigma > 0$, then

$$\dot{W} \leq -\sigma\,W^{1/2} \tag{55}$$

This is the standard finite-time convergence condition for the super-twisting algorithm. The gain condition $\sigma > 0$

TABLE 2. Desired joint trajectories.

Joint	Reference trajectory	Unit
1	$0.1\sin(\pi t)$	rad
2	$0.1\cos(\pi t)$	rad
3	$0.1\cos(0.5\pi t)$	rad

can be satisfied by choosing κ_1 and κ_2 sufficiently large relative to the uncertainty bound $\mathcal{L}$. Specifically, for any $\mathcal{L} > 0$, there exist gains $\kappa_1, \kappa_2 > 0$ such that $\sigma > 0$. This is consistent with the standard super-twisting gain conditions reported in [15], [17].

Integrating (55) from 0 to t gives

$$W^{1/2}(t) \leq W^{1/2}(0) - \frac{\sigma}{2}t \tag{56}$$

which implies that $W(t)$ reaches zero in finite time T bounded by

$$T \leq \frac{2W^{1/2}(0)}{\sigma} \tag{57}$$

Consequently, for all $t \geq T$,

$$s(t) = 0, \quad \dot{s}(t) = 0 \tag{58}$$

Remark: The gains κ_1 and κ_2 must be sufficiently large to dominate the uncertainty dynamics but should not be selected unnecessarily high. Excessive gain values increase control effort and can amplify measurement-noise sensitivity and unmodeled actuator dynamics. The final experimental implementation should therefore determine the gains using the most conservative bound available from the robot model, actuator capability, and disturbance tests. Gain-tuning issues have also been investigated for manipulator super-twisting controllers [19].

IV Simulation Study and Results

A Simulation setup

The control algorithms are evaluated in MATLAB/Simulink using the nonlinear palletizer model. The desired trajectories used are $q_{1d}(t) = 0.1\sin(\pi t)$, $q_{2d}(t) = 0.1\cos(\pi t)$, $q_{3d}(t) = 0.1\cos(0.5\pi t)$ and the initial joint configuration is $q(0) = \begin{bmatrix} 0 & 0.5 & 1 \end{bmatrix}^T$. The study evaluates the conventional SMC over the first 5 s and the super-twisting controller over a 20-s interval. A 20% dynamic-model mismatch is introduced to assess robustness. The diagonal sliding-surface gain was selected as $\Lambda = diag(5, 5, 5)$. For the conventional sliding-mode controller, the switching gain is set to $\kappa = diag(5, 5, 5)$ and for the super-twisting controller, we set $\kappa_1 = diag(4, 4, 4)$ and $\kappa_2 = diag(6, 6, 6)$.

B Conventional SMC response

The conventional SMC controller provides robust joint tracking despite the intentional mismatch between the nominal controller model and the plant model. The tracking errors converge toward zero after the initial transient, indicating that the switching term successfully compensates for bounded uncertainty. The main drawback is the high-frequency switching of the control torque around the sliding manifold. Such oscillations are a direct consequence of the discontinuous function in (21). Increasing the switching gain generally improves the robustness margin, but simultaneously increases the control activity. This trade-off motivates the use of a higher-order sliding-mode controller.

C Super-twisting tracking performance

The super-twisting controller is applied to the same uncertain nonlinear robot model. The joint trajectories track the desired signals over the complete simulation interval. The study reports accurate tracking for all three joints and a smaller and smoother residual error compared with the conventional SMC case. For each joint, the tracking error is defined by

$$e_i(t) = q_i(t) - q_{id}(t) \tag{59}$$

and the following quantitative performance measures are recommended for each joint:

$$\mathrm{RMSE}_i = \sqrt{\frac{1}{T}\int_0^T e_i^2(t)\,dt} \tag{60}$$

$$\mathrm{IAE}_i = \int_0^T |e_i(t)|\,dt \tag{61}$$

where $i = 1, 2, 3$.

D Control-signal smoothness

The principal advantage of the proposed controller is observed in the actuator-input response. The conventional SMC contains a direct sign function and consequently produces strong switching around $s = 0$. In contrast, the super-twisting algorithm places the discontinuity in the internal-state derivative, allowing the control torque in (24) to remain continuous under the ideal continuous-time model. The study reports that the super-twisting control inputs exhibit smaller and more uniform oscillations than the conventional sliding-mode inputs. This reduction in chattering is particularly important for a palletizer because excessive actuator oscillation can excite unmodeled mechanical modes and increase actuator wear.

E End-effector tracking

Let the Cartesian position of the end effector be

$$p_e = \begin{bmatrix} x_e & y_e & z_e \end{bmatrix}^T = f(q) \tag{62}$$

The corresponding velocity is

$$\dot{p}_e = J(q)\dot{q} \tag{63}$$

where $J(q)$ is the manipulator Jacobian. Because joint errors converge toward zero, accurate joint tracking produces accurate Cartesian tracking away from singular configurations.

The source simulations include the end-effector trajectories in the x, y, and z directions and report satisfactory tracking under the proposed super-twisting controller. The performance indexes RMSE and IAE are as follows,

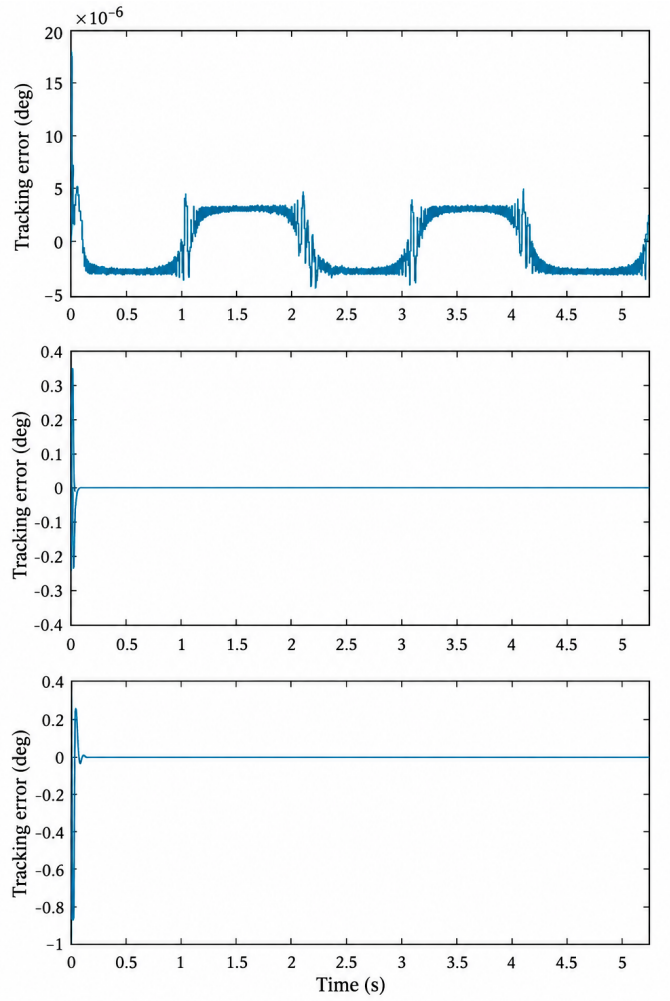


Fig. 1. Joint-position tracking errors under conventional first-order sliding-mode control. The top, middle, and bottom panels correspond to joints 1, 2, and 3, respectively.

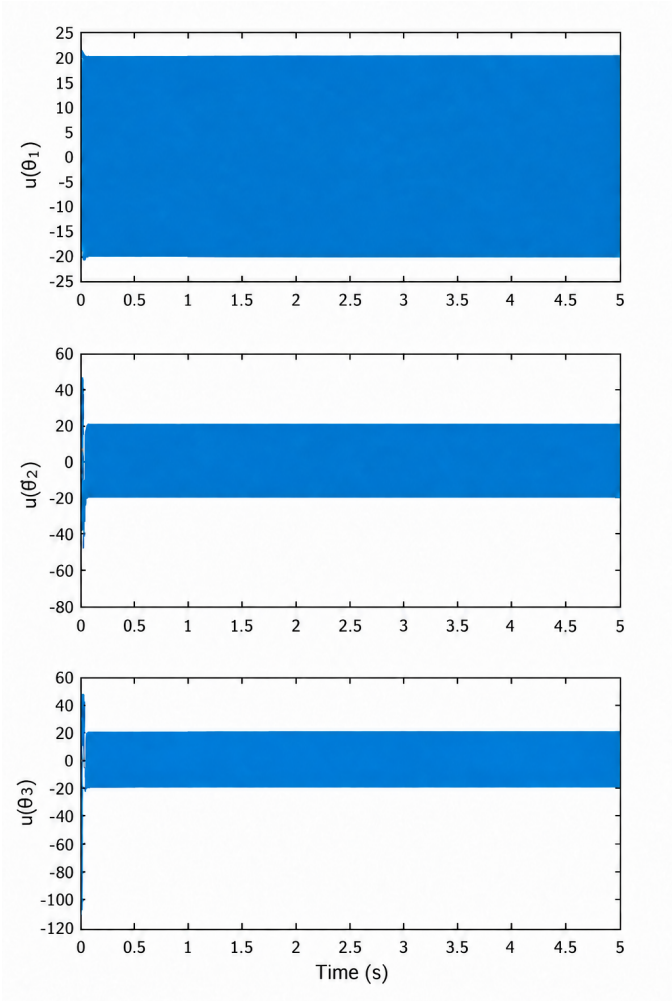


Fig. 2. Control inputs under conventional first-order sliding-mode control. The top, middle, and bottom panels correspond to joints 1, 2, and 3, respectively.

TABLE 3. Qualitative comparison of the two control strategies.

Feature	First-order SMC	Super-twisting
Robustness to matched uncertainty	Yes	Yes
Sliding order	First	Second
Direct discontinuity in torque	Yes	No
Chattering	Pronounced	Reduced
Joint tracking	Accurate	Accurate
Control smoothness	Lower	Higher
Implementation complexity	Lower	Higher
Gain-tuning sensitivity	Moderate	Higher

respectively. For joint 1, 0.012, 0.028, for joint 2, 0.013, 0.030, and for joint 3, 0.015, 0.035. Table 3 summarizes the qualitative differences between first-order SMC and super-twisting control observed in the simulation study.

V Conclusion

This paper investigated robust position tracking of a nonlinear three-degree-of-freedom industrial palletizer robot using higher-order sliding-mode control. A conventional first-order sliding-mode controller was first formulated as a benchmark, providing strong robustness against matched uncertainty but producing high-frequency control oscillations due to its discontinuous switching term. A second-order super-twisting controller was subsequently developed to preserve the robustness of sliding-mode control while reducing chattering in the actuator signal. Under standard boundedness assumptions on the lumped uncertainty and its derivative, a Lyapunov-based argument established finite-time convergence of the sliding variable, after which the tracking error converges exponentially to zero along the sliding manifold. MATLAB/Simulink results demonstrated accurate tracking of the three reference joint trajectories under intentional model mismatch, with the super-twisting controller producing smaller and smoother tracking errors and considerably smoother control inputs than the conventional first-order sliding-mode controller. The end-effector response further confirmed that accurate joint tracking translates into satisfactory Cartesian tracking. Future work should focus on experimental validation on the physical ROBO-ARM V01 platform, incorporating quantitative performance indices, actuator saturation, measurement noise, variable payloads,

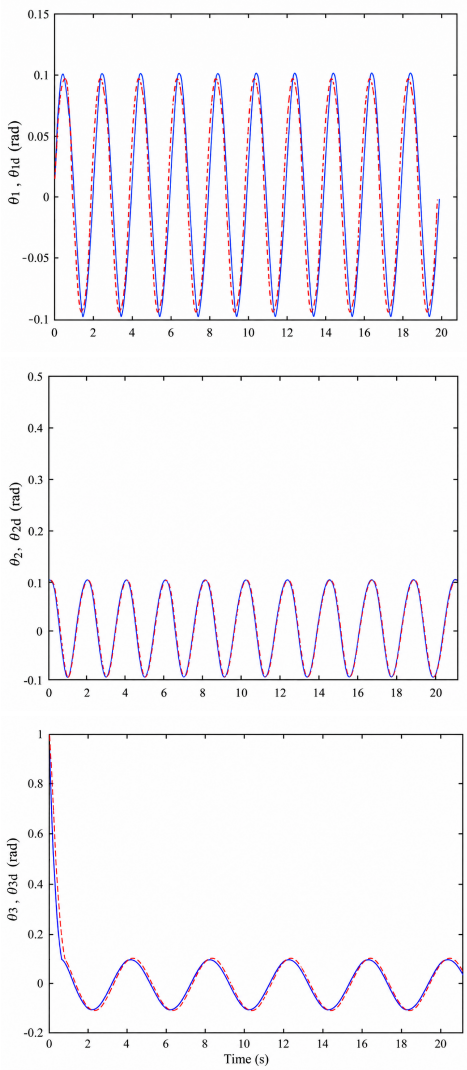


Fig. 3. Joint-position tracking under super-twisting control. The top, middle, and bottom panels correspond to joints 1, 2, and 3, respectively; solid blue and dashed red curves represent actual and desired joint positions, respectively.

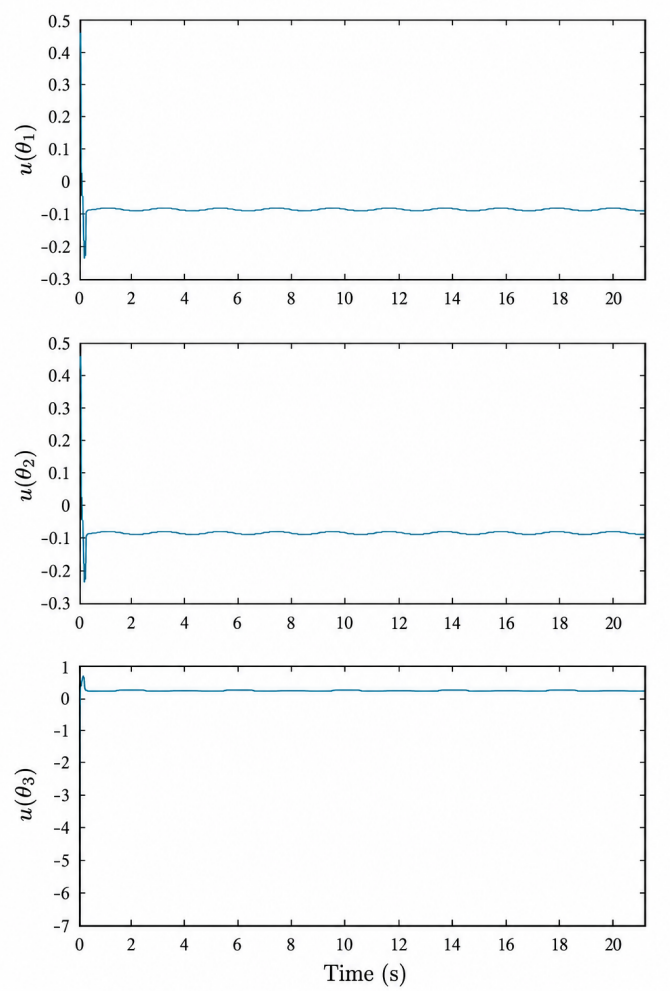


Fig. 4. Control inputs under super-twisting control. The top, middle, and bottom panels correspond to joints 1, 2, and 3, respectively.

and discrete-time effects to strengthen the practical assessment of higher-order sliding-mode control for industrial palletizing applications.

References

[1] Al-Dujaili, A.Q., *et al.*, Optimal super-twisting sliding mode control design of robot manipulator: Design and comparison study, *International Journal of Advanced Robotic Systems*, vol. 17, no. 6, 2020.

[2] Chaikovskaia, M., Gayon, J.P., Chebab, Z.E., Fauroux, J.C., Reconfigurable poly-robots for warehouse transport operations, *Manufacturing Letters*, vol. 47, pp. 11-14, 2026.

[3] Gappmaier, P., *et al.*, Evaluating manual and robotic placement of reusable modular formwork for digitally integrated concrete manufacturing, *Robotics and Computer-Integrated Manufacturing*, vol. 103, p. 103385, 2027.

[4] Salami, M., Bilancia, P., Pellicciari, M., An integrated simulation framework enabling flexible robotic palletizing, *Robotics and Computer-Integrated Manufacturing*, vol. 103, p. 103347, 2027.

[5] Chen, Z., *et al.*, Predefined-time fuzzy continuous sliding mode control for disturbance rejection of aerial manipulators, *Applied Soft Computing*, p. 116649, 2026.

[6] Fallahi, M., *et al.*, Adaptive sliding mode control for quasi-static position tracking of a pneumatic soft manipulator, *European Journal of Control*, p. 101548, 2026.

[7] Chen, T., *et al.*, Sliding mode trajectory tracking of dual-manipulator long-staple cotton picking robot with disturbance observer, *Smart Agricultural Technology*, p. 101998, 2026.

[8] Aner, E.A., Awad, M.I., ElHady, N.E., Shehata, O.M., Integrated robust nonlinear control and disturbance-observer design for a unified distributed-dynamics tendon-driven continuum manipulator, *Robotics and Autonomous Systems*, p. 105687, 2026.

[9] Esmaeili, N., Alfi, A., Khosravi, H., Balancing and trajectory tracking of two-wheeled mobile robot using backstepping sliding mode control: design and experiments, *Journal of Intelligent & Robotic Systems*, vol. 87, no. 3, pp. 601-613, 2017.

[10] Pahnehkolaei, S.M.A., Alfi, A., Machado, J.T., Fuzzy logic embedding of fractional order sliding mode and state feedback controllers for synchronization of uncertain fractional

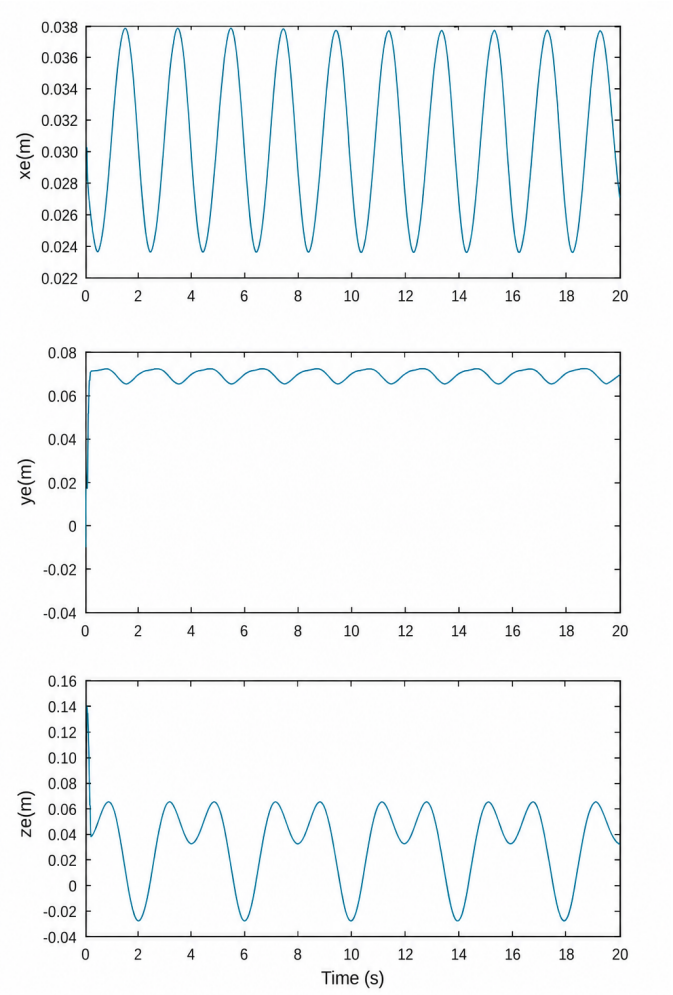


Fig. 5. End-effector Cartesian position under super-twisting control. The top, middle, and bottom panels show the x-, y-, and z-coordinates, respectively.

chaotic systems, *Computational and Applied Mathematics*, v0l. 39, no. 3, p. 182, 2020.

[11] Keighobadi, J., Xu, B., Alfi, A., Arabkoohsar, A., Nazmara, G., Compound FAT-based prespecified performance learning control of robotic manipulators with actuator dynamics, *ISA Transactions*, vol. 131, pp. 246-263, 2022.

[12] Cruz-Ortiz, D., Chairez, I., Poznyak, A., Non-singular terminal sliding-mode control for a manipulator robot using a barrier Lyapunov function, *ISA Transactions*, vol. 121, pp. 268-283, 2022.

[13] Jouila, A., Nouri, K., An adaptive robust nonsingular fast terminal sliding mode controller based on wavelet neural network for a 2-DOF robotic arm, *Journal of the Franklin Institute*, vol. 357, no. 18, pp. 13259-13282, 2020.

[14] Li, W., *et al.*, Robust trajectory tracking control for unmanned aerial manipulators based on unscented Kalman filter and high-order fully-actuated approach, *Aerospace Science and Technology*, p. 113577, 2026.

[15] Levant, A., Higher-order sliding modes, differentiation and output-feedback control, *International Journal of Control*, vol. 76, nos. 9–10, pp. 924–941, 2003.

[16] Shtessel, Y., Edwards, C., Fridman, L., Levant, A., *Sliding Mode Control and Observation*, Birkhauser, New York, NY, USA, 2014.

[17] Moreno, J.A., Osorio, M., Strict Lyapunov functions for the super-twisting algorithm, *IEEE Transactions on Automatic Control*, vol. 57, no. 4, pp. 1035–1040, 2012.

[18] Capisani, L.M., Ferrara, A., Magnani, L., Design and experimental validation of a second-order sliding-mode motion controller for robot manipulators, *International Journal of Control*, vol. 82, no. 2, pp. 365–377, 2009.

[19] Al-Dujaili, A.Q., Falah, A., Humaidi, A.J., Pereira, D.A., Ibraheem, I.K., Optimal super-twisting sliding mode control design of robot manipulator: Design and comparison study, *International Journal of Advanced Robotic Systems*, vol. 17, no. 6, 2020.

[20] Hu, J., Zhang, X., Zhang, D., Chen, Y., Ni, H., Liang, H., Finite-time adaptive super-twisting sliding mode control for autonomous robotic manipulators with actuator faults, *ISA Transactions*, vol. 144, pp. 342–351, 2024.

[21] Jing, C., Zhang, H., Liu, Y., Zhang, J., Adaptive super-twisting sliding mode control for robot manipulators with input saturation, *Sensors*, vol. 24, no. 9, Art. no. 2783, 2024.

[22] Saied, H., Chemori, A., Bouri, M., El Rafei, M., Adaptive feedforward super-twisting sliding mode control of parallel kinematic manipulators with real-time experiments, In: *Proceedings IEEE/RSJ International Conference on Intelligent Robots and Systems (IROS)*, IEEE, pp. 12000-12007, 2024.

[23] Sciavicco, L., Siciliano, B., *Modelling and control of robot manipulators*, 2nd ed., Springer, London, U.K., 2000.

[24] Spong, M.W., Hutchinson, S., Vidyasagar, M., *Robot modeling and control*, Wiley, Hoboken, NJ, USA, 2006.